Supporting Information

Highly efficient and robust nickel phosphides as bifunctional electrocatalysts for overall water-splitting

Jiayuan Li, [†,#] *Jing Li,* [†,#] *Xuemei Zhou,*[†] *Zhaoming Xia,* [†] *Wei Gao,*[†] *Yuanyuan Ma,* [†,*] *and Yongquan Qu*[†, ‡,*]

[†] *Center for Applied Chemical Research, Frontier Institute of Science and Technology, and State Key Laboratory for Mechanical Behavior of Materials, Xi'an Jiaotong University, Xi'an Jiaotong University, Xi'an, 710049, China.*

[‡] *MOE Key Laboratory for Nonequilibrium Synthesis and Modulation of Condensed Matter, Xi'an Jiaotong University, Xi'an, 710049, China.*

E-mail: yongquan@mail.xjtu.edu.cn, yyma@mail.xjtu.edu.cn

# Authors contributed equally.

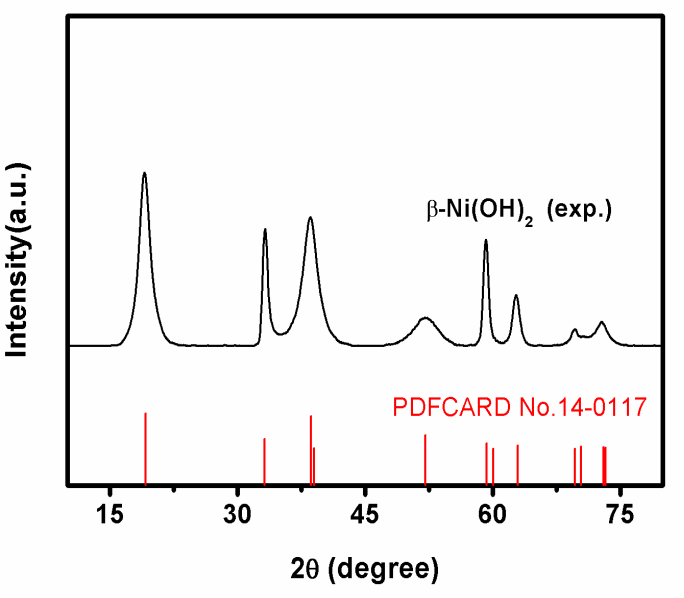

Figure S1. Powder XRD pattern of the as-prepared β-$Ni(OH)_2$ nanoplate precursor.

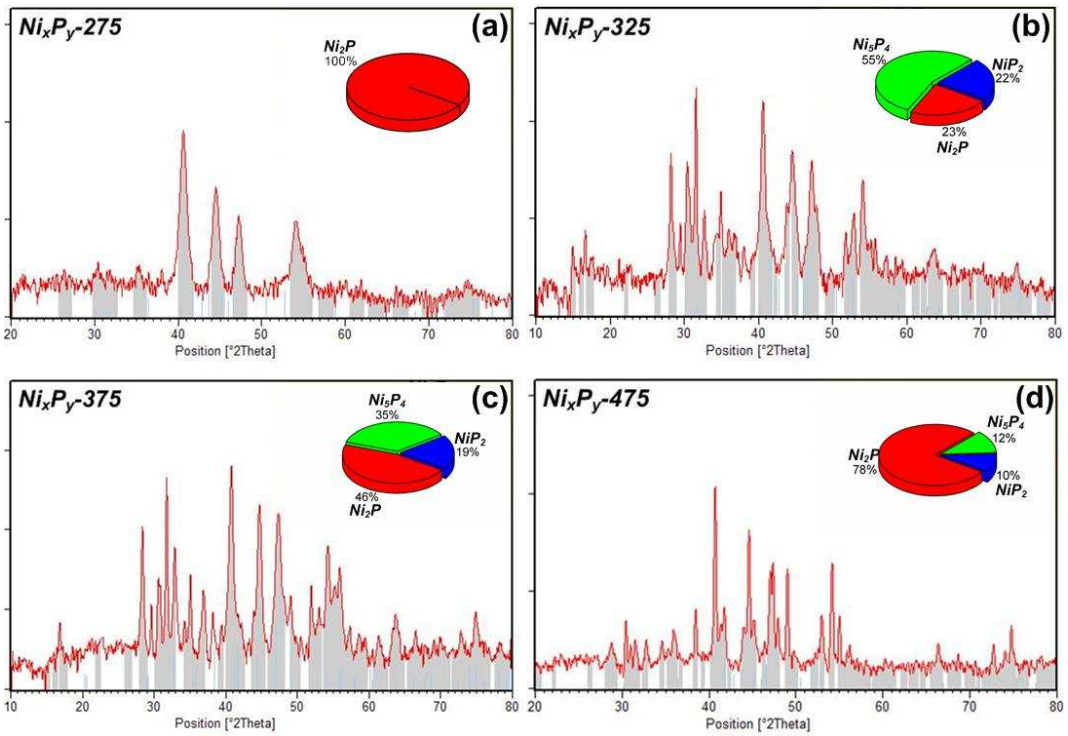

Figure S2. Phase composition analysis of the Ni_xP_y-T catalysts: **(a)** Ni_xP_y-275 **(b)** Ni_xP_y-325 **(c)** Ni_xP_y-375 **(d)** Ni_xP_y-475.

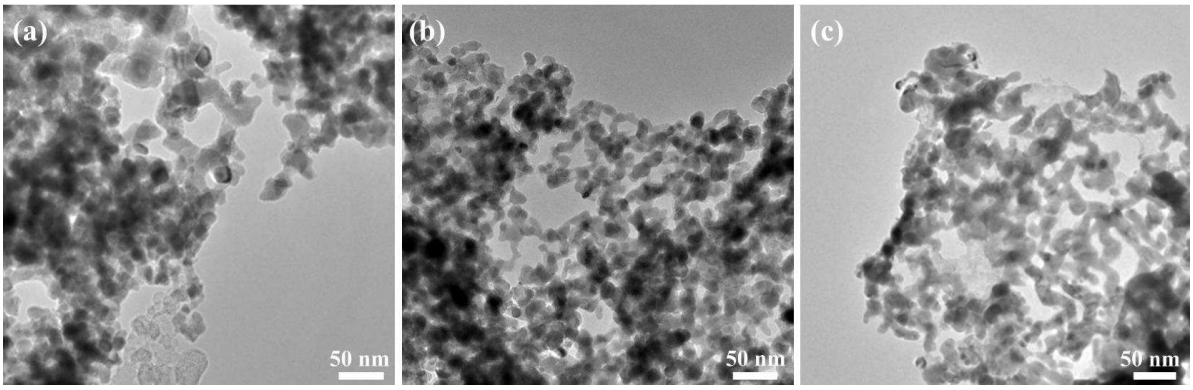

Figure S3. TEM image of as-prepared **(a)** Ni_xP_y-275, **(b)** Ni_xP_y-375 and **(c)** Ni_xP_y-475.

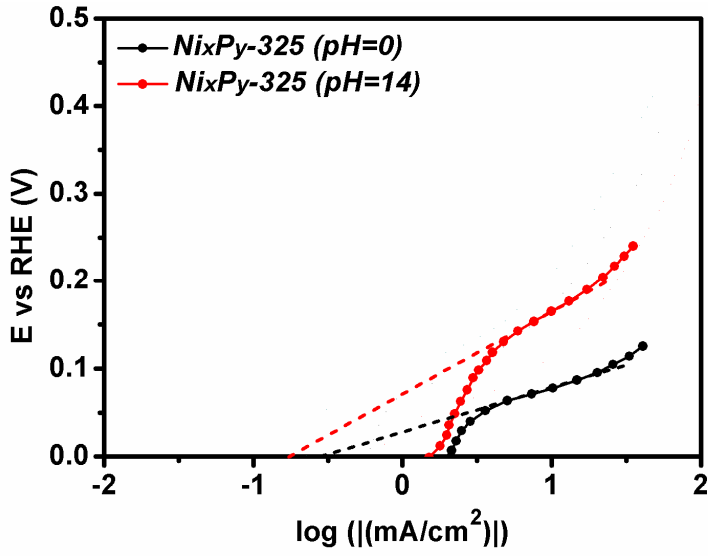

Figure S4. Derived exchange current densities of the Ni_xP_y-325 catalysts in various pH environments by applying extrapolation method to the Tafel plots.

TOF calculation:

An electrochemical cyclic voltammetry test was employed to quantify the active sites of the Ni_xP_y-T nanocatalysts in 1.0 M PBS (pH=7.0) with a potential window from −0.2 to 0.6 V *vs* RHE at a scan rate of 50 mV/s (Figure S3).[1] Assuming one electron redox process, the integrated charge over the whole potential range was divided by two. Then, the value was divided by the Faraday constant to get the number of active sites for different samples. The turnover frequency (s^{-1}) can be estimated according to this equation[2]:

$$\mathrm{TOF} = I/2nF$$

where I represents the current density for different samples during the LSV measurement in 0.5 M H_2SO_4, F is the Faraday constant (C/mol), and n is the number of the active sites (mol) for different samples.

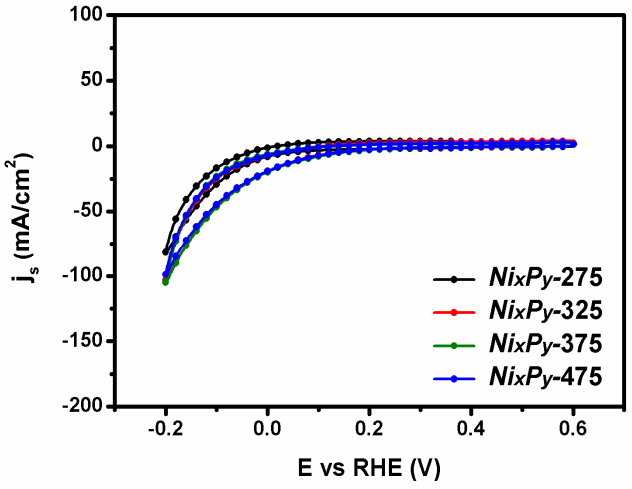

Figure S5. The cyclic voltammetries for the Ni_xP_y-T catalysts in 1.0 M PBS at a scan rate of 50 mV/s.

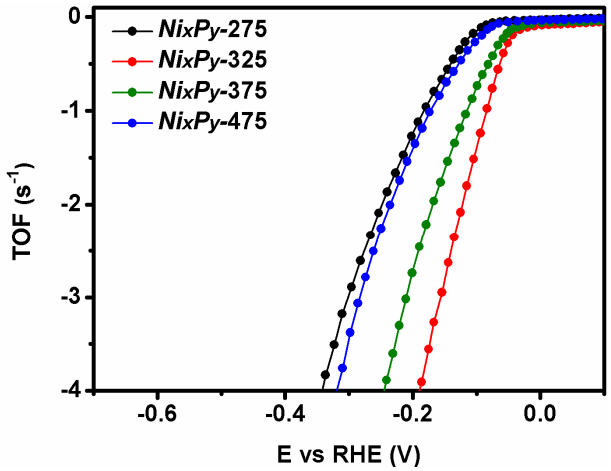

Figure S6. The calculated TOF curves for the Ni_xP_y-T catalysts in 0.5 M H_2SO_4 electrolyte.

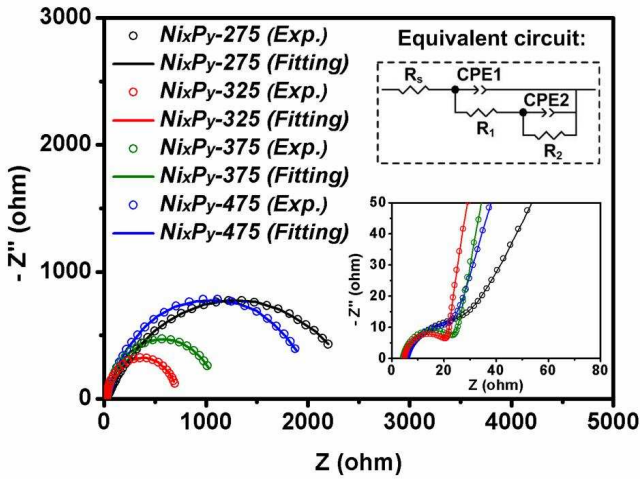

Figure S7. Nyquist plots for the Ni_xP_y-T catalysts in 0.5 M H_2SO_4 electrolyte. The scattered symbols represent the experimental results and the solid lines are simulation fitted results. The inset at the top shows the equivalent circuit for the simulation. Electrochemical impedance spectroscopy of the catalysts was carried out on an electrochemistry workstation (AUTOLAB PGSTAT204) under an overpotential of 10 mV within a frequency window of 100 kHz to 0.1 Hz.

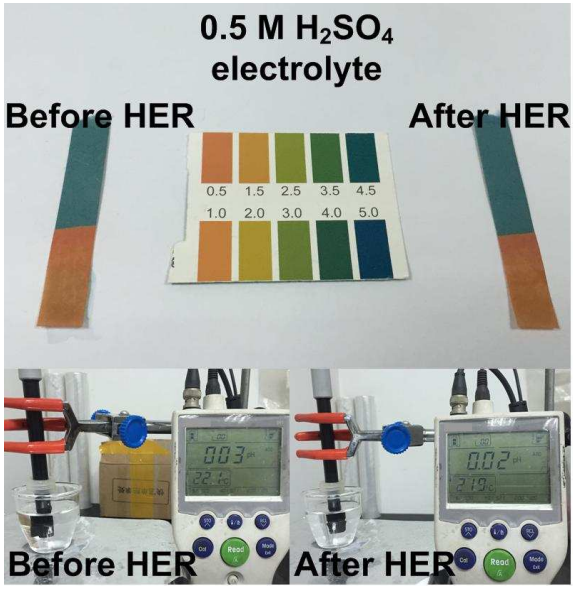

Figure S8. The pH monitoring in 0.5 M H_2SO_4 electrolyte after the HER catalytic durability measurement for the Ni_xP_y-325.

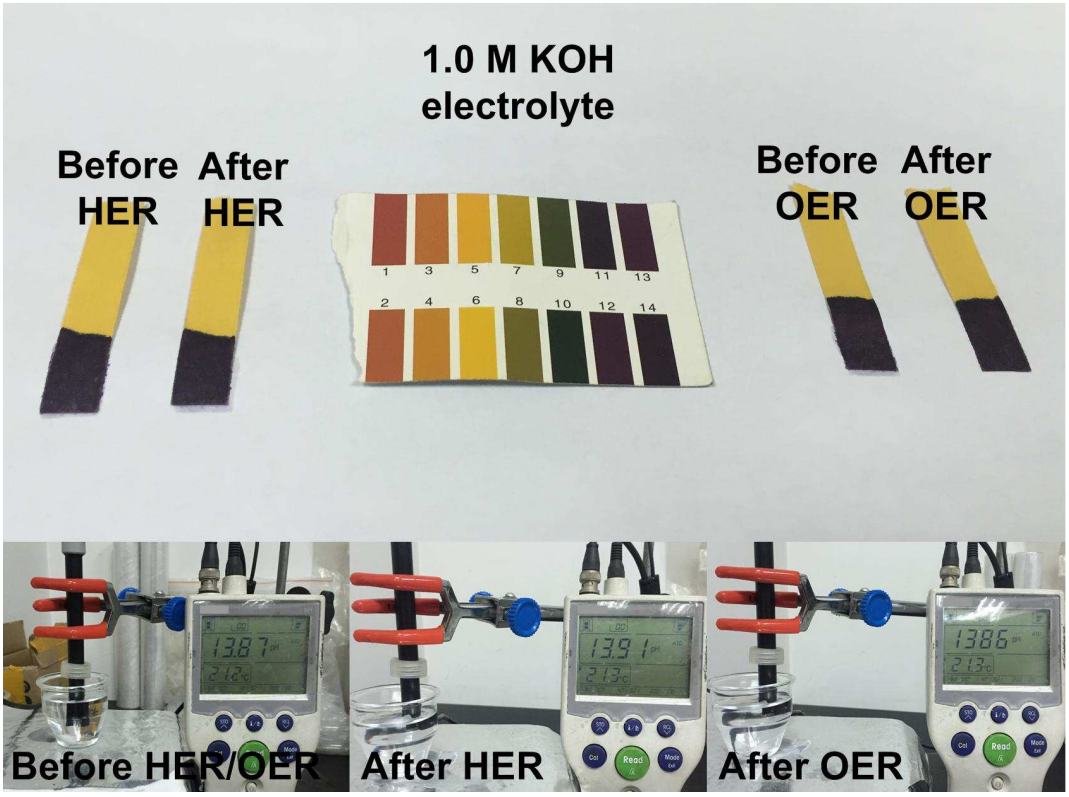

Figure S9. The pH monitoring in 1.0 M KOH electrolyte after the HER and OER catalytic durability measurement for the Ni_xP_y-325.

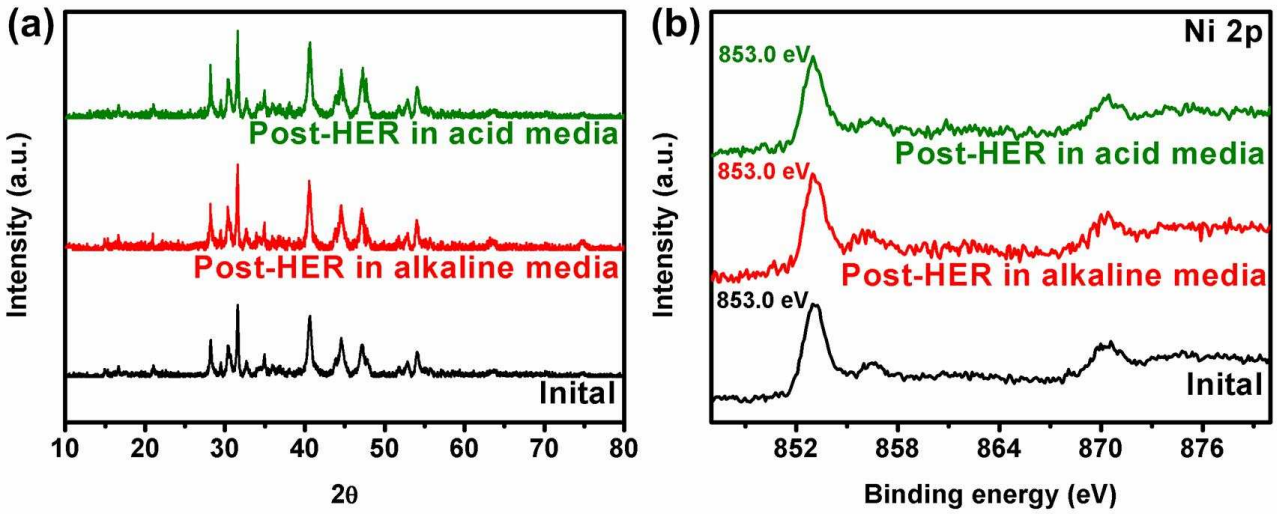

Figure S10. The XRD patterns **(a)** and XPS spectra of Ni 2p region **(b)** for the Ni_xP_y-325 catalyst before and after HER in alkaline (1.0 M KOH) and acid (0.5 M H_2SO_4) media respectively.

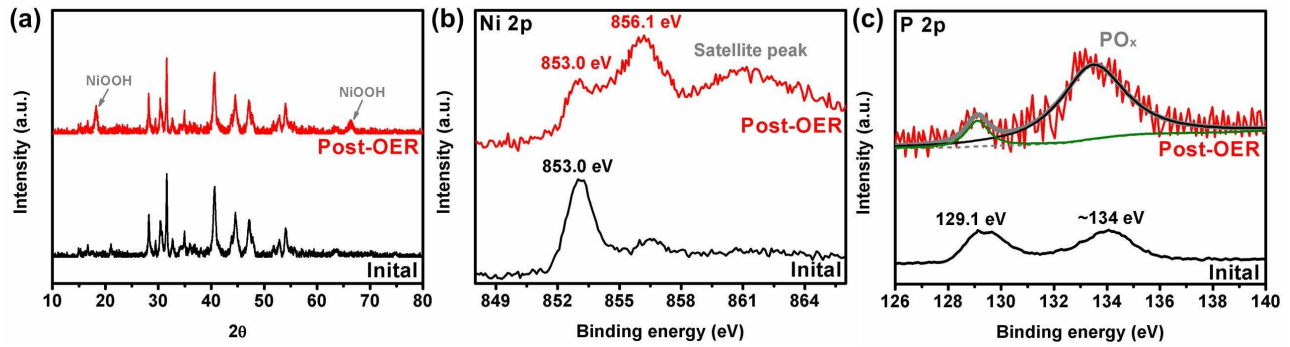

Figure S11. (a) XRD patterns of the Ni_xP_y-325 catalyst before and after OER in 1.0 M KOH. The XPS spectra of **(b)** Ni 2p and **(c)** P 2p region of the Ni_xP_y-325 catalyst before and after OER in 1.0 M KOH.

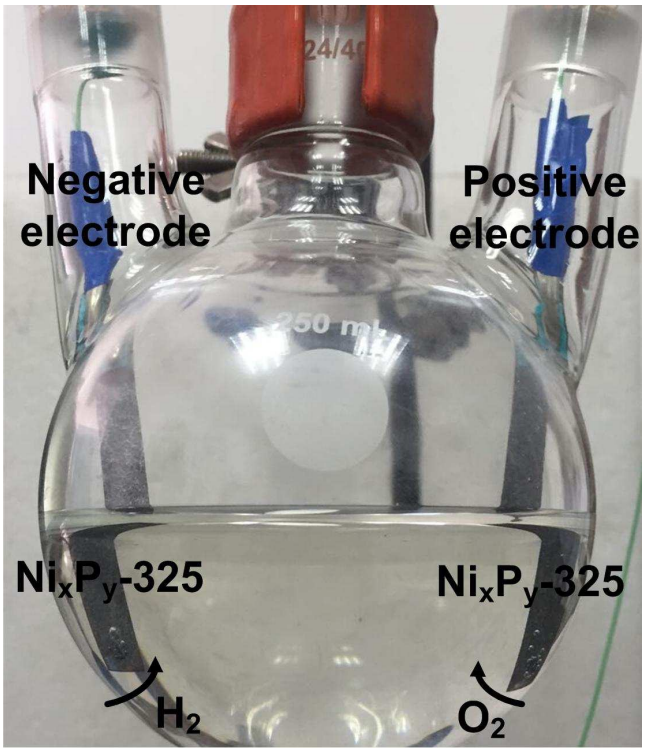

Figure S12. A photograph of the Ni_xP_y-325 ‖ Ni_xP_y-325 water electrolyzer.

Table S1. Comparison of HER performance of Ni_xP_y-325 in acid environment with the nickel- and cobalt-based phosphides.

Catalyst	η_{20} (mV)	Tafel slope (mV/dec)	Exchange current density (mA/cm^2)	References
Ni_2P nanoparticles	130	46	3.3×10^{-3}	3
Ni_5P_4 nanocrystals	175	42	0.057	4
$Ni_{12}P_5$ nanoparticles	141	63	–	5
Ni_5P4-Ni_2P nanosheet	140	79.1	0.116	6
Ni_2P NPs/Ti	138	60	–	7
Ni_2P/C	115	54	–	8
CoP nanoparticles	85	50	0.14	9
CoP nanowires	100	51	0.288	2
CoP/CNT	160	54	0.13	10
Co_2P nanorods	167	51.7	–	11
Ni_5P_4 nanocrystals	35	33	–	12
Ni_5P_4 films	~ 180	~ 40	–	13
Ni_xP_y-325	**62**	**46.1**	**0.275**	**This work**

Table S2. Comparison of HER performance of Ni_xP_y-325 in acid environment with other non-Pt HER catalysts.

Catalyst	η_{20} (mV)	Tafel slope (mV/dec)	Exchange current density (mA/cm^2)	References
Defect-rich MoS_2 nanosheets	214	50	8.9×10^{-3}	14
MoS_2/rGO	176	41	−	15
MoS@Au	−	69	9.3×10^{-3}	16
WS_2 nanosheets	275	55	−	17
MoP	151	54	0.086	18
$CoSe_2$	−	42.4	6.5×10^{-5}	19
Ni-Mo nanopower	80	−	−	20
Bulk Mo_2C	224	56	1.3×10^{-3}	21
Cu_2MoS_4	−	95	−	22
$Fe_{0.9}Co_{0.1}S_2$/CNT	120	46	−	23
FeP nanosheets	~300	67	−	24
$Co_{0.6}Mo_{1.4}N_2$	267	−	2.3×10^{-4}	25
Ni_xP_y-325	**62**	**46.1**	**0.275**	**This work**

Table S3. Comparison of HER performance of Ni_xP_y-325 in alkaline environment with other non-precious HER catalysts.

Catalyst	η_{20} (mV)	Tafel slope (mV/dec)	References
CoP nanowire	335	129	2
Co-NRCNTs	476	−	26
$Ni_{0.33}Co_{0.67}S_2$	129	118	27
$NiCo_2S_4$	194	141	28
CoO_x/CN	352	114	29
Ni_5P_4 films	~ 180	~ 53	13
Ni_2P	255	−	30
NiFe LDH/NF	250	−	31
MoC_x/C	> 175	59	32
Ni_2P nanoparticles	205	−	3
Ni_xP_y-325	**160**	**107.3**	**This work**

Table S4. Comparison of OER performance of Ni_xP_y-325 in alkaline environment with the state-of the-art OER catalysts

Catalyst	Electrolyte	η_{10} (mV)	References
Ni–Co binary oxides	1.0 M KOH	325	33
$Co_{0.5}Fe_{0.5}S$@N-MC	1.0 M KOH	410	34
CoNi SUNOE	1.0 M KOH	450	35
NiCo LDH	1.0 M KOH	367	36
$Ni_xCo_{3-x}O_4$ NWs/Ti	1.0 M KOH	370	37
Co_3O_4/ $NiCo_2O_4$ DSNCs	1.0 M KOH	340	38
Ni_5P_4 films	1.0 M KOH	290	13
Ni_2P	1.0 M KOH	290	30
Fe-Ni oxide	1.0 M KOH	>375	39
$CoSe_2$	0.1 M KOH	320	40
NiCo-NS	1.0 M KOH	334	41
Co-P film	1.0 M KOH	345	42
$MnCo_2O_x$	1.0 M KOH	> 410	43
Ni_xP_y-325	**1.0 M KOH**	**320**	**This work**

Table S5. Fitting parameter values of the EIS data of Ni_xP_y-T catalysts for HER.

Sample	R_s (Ω)	R_1 (Ω)	n_1	CPE_1	R_2 (Ω)	n_2	CPE_2	C_{DL} (F)
Ni_xP_y-275	5.5	29.9	0.89	4.5×10^{-5}	2501	0.70	9.0×10^{-4}	1.81×10^{-5}
Ni_xP_y-325	4.8	17.9	0.90	5.1×10^{-5}	699	0.95	8.9×10^{-4}	1.91×10^{-5}
Ni_xP_y-375	4.2	21.8	0.87	4.1×10^{-5}	1105	0.90	7.9×10^{-4}	1.94×10^{-5}
Ni_xP_y-475	5.8	24.1	0.85	8.0×10^{-5}	2047	0.83	6.1×10^{-4}	1.99×10^{-5}

References:

1. Merki, D.; Fierro, S.; Vrubel, H.; Hu, X. Amorphous Molybdenum Sulfide Films as Catalysts for Electrochemical Hydrogen Production in Water. *Chem. Sci.* **2011**, *2*, 1262-1267.
2. Tian, J.; Liu, Q.; Asiri, A. M.; Sun, X. Self-Supported Nanoporous Cobalt Phosphide Nanowire Arrays: An Efficient 3D Hydrogen-Evolving Cathode over the Wide Range of pH 0-14. *J. Am. Chem. Soc.* **2014**, *136*, 7587-7590.
3. Popczun, E. J.; McKone, J. R.; Read, C. G.; Biacchi, A. J.; Wiltrout, A. M.; Lewis, N. S.; Schaak, R. E. Nanostructured Nickel Phosphide as An Electrocatalyst for the Hydrogen Evolution Reaction. *J. Am. Chem. Soc.* **2013**, *135*, 9267-9270.
4. Pan, Y.; Liu, Y.; Zhao, J.; Yang, K.; Liang, J.; Liu, D.; Hu, W.; Liu, D.; Liu, Y.; Liu, C. Monodispersed Nickel Phosphide Nanocrystals with Different Phases: Synthesis, Characterization and Electrocatalytic Properties for Hydrogen Evolution. *J. Mater. Chem. A* **2015**, *3*, 1656-1665.
5. Huang, Z.; Chen, Z.; Chen, Z.; Lv, C.; Meng, H.; Zhang, C. $Ni_{12}P_5$ Nanoparticles as An Efficient Catalyst for Hydrogen Generation via Electrolysis and Photoelectrolysis. *ACS Nano* **2014**, *8*, 8121-8129.
6. Wang, X.; Kolen'ko, Y. V.; Bao, X. Q.; Kovnir, K.; Liu, L. One-Step Synthesis of Self-Supported Nickel Phosphide Nanosheet Array Cathodes for Efficient Electrocatalytic Hydrogen Generation. *Angew. Chem. Int. Ed.* **2015**, *54*, 8188-8192.
7. Pu, Z.; Liu, Q.; Tang, C.; Asiri, A. M.; Sun, X. Ni_2P Nanoparticle Films Supported on A Ti Plate as An Efficient Hydrogen Evolution Cathode. *Nanoscale* **2014**, *6*, 11031-11034.
8. Bai, Y.; Zhang, H.; Li, X.; Liu, L.; Xu, H.; Qiu, H.; Wang, Y. Novel Peapod-Like Ni_2P Nanoparticles with Improved Electrochemical Properties for Hydrogen Evolution and Lithium Storage. *Nanoscale* **2015**, *7*, 1446-1453.
9. Popczun, E. J.; Read, C. G.; Roske, C. W.; Lewis, N. S.; Schaak, R. E. Highly Active Electrocatalysis of the Hydrogen Evolution Reaction by Cobalt Phosphide Nanoparticles. *Angew. Chem.* **2014**, *126*, 5531-5534.
10. Liu, Q.; Tian, J.; Cui, W.; Jiang, P.; Cheng, N.; Asiri, A. M.; Sun, X. Carbon Nanotubes Decorated with CoP Nanocrystals: A Highly Active Non-Noble-Metal Nanohybrid Electrocatalyst for Hydrogen Evolution. *Angew. Chem.* **2014**, *126*, 6828-6832.
11. Huang, Z.; Chen, Z.; Chen, Z.; Lv, C.; Humphrey, M. G.; Zhang, C. Cobalt Phosphide Nanorods as An Efficient Electrocatalyst for the Hydrogen Evolution Reaction. *Nano Energy* **2014**, *9*, 373-382.
12. Laursen, A.; Patraju, K.; Whitaker, M.; Retuerto, M.; Sarkar, T.; Yao, N.; Ramanujachary, K.; Greenblatt, M.; Dismukes, G. Nanocrystalline Ni_5P_4: A Hydrogen Evolution Electrocatalyst of Exceptional Efficiency in Both Alkaline and Acidic Media. *Energy Environ. Sci.* **2015**, *8*, 1027-1034.
13. Ledendecker, M.; Krick Calderón, S.; Papp, C.; Steinrück, H. P.; Antonietti, M.; Shalom, M. The Synthesis of Nanostructured Ni_5P_4 Films and Their Use as A Non-Noble Bifunctional Electrocatalyst for Full Water Splitting. *Angew. Chem.* **2015**, *127*, 12538-12542.
14. Xie, J.; Zhang, H.; Li, S.; Wang, R.; Sun, X.; Zhou, M.; Zhou, J.; Lou, X. W. D.; Xie, Y. Defect-Rich MoS_2 Ultrathin Nanosheets with Additional Active Edge Sites for Enhanced Electrocatalytic Hydrogen Evolution. *Adv. Mater.* **2013**, *25*, 5807-5813.
15. Li, Y.; Wang, H.; Xie, L.; Liang, Y.; Hong, G.; Dai, H. MoS_2 Nanoparticles Grown on Graphene: An Advanced Catalyst for the Hydrogen Evolution Reaction. *J. Am. Chem. Soc.* **2011**, *133*, 7296-7299.
16. Wang, T.; Liu, L.; Zhu, Z.; Papakonstantinou, P.; Hu, J.; Liu, H.; Li, M. Enhanced Electrocatalytic Activity for Hydrogen Evolution Reaction from Self-Assembled Monodispersed Molybdenum Sulfide Nanoparticles on An Au Electrode. *Energy Environ. Sci.* **2013**, *6*, 625-633.
17. Voiry, D.; Yamaguchi, H.; Li, J.; Silva, R.; Alves, D. C.; Fujita, T.; Chen, M.; Asefa, T.; Shenoy, V. B.; Eda, G. Enhanced Catalytic Activity in Strained Chemically Exfoliated WS_2 Nanosheets for Hydrogen Evolution. *Nat. Mater.* **2013**, *12*, 850-855.

18. Xiao, P.; Sk, M. A.; Thia, L.; Ge, X.; Lim, R. J.; Wang, J.-Y.; Lim, K. H.; Wang, X. Molybdenum Phosphide as An Efficient Electrocatalyst for the Hydrogen Evolution Reaction. *Energy Environ. Sci.* **2014**, *7*, 2624-2629.
19. Kong, D.; Cha, J. J.; Wang, H.; Lee, H. R.; Cui, Y. First-Row Transition Metal Dichalcogenide Catalysts for Hydrogen Evolution Reaction. *Energy Environ. Sci.* **2013**, *6*, 3553-3558.
20. McKone, J. R.; Sadtler, B. F.; Werlang, C. A.; Lewis, N. S.; Gray, H. B. Ni–Mo Nanopowders for Efficient Electrochemical Hydrogen Evolution. *ACS Catal.* **2013**, *3*, 166-169.
21. Vrubel, H.; Hu, X. Molybdenum Boride and Carbide Catalyze Hydrogen Evolution in Both Acidic and Basic Solutions. *Angew. Chem.* **2012**, *124*, 12875-12878.
22. Tran, P. D.; Nguyen, M.; Pramana, S. S.; Bhattacharjee, A.; Chiam, S. Y.; Fize, J.; Field, M. J.; Artero, V.; Wong, L. H.; Loo, J. Copper Molybdenum Sulfide: A New Efficient Electrocatalyst for Hydrogen Production from Water. *Energy Environ. Sci.* **2012**, *5*, 8912-8916.
23. Wang, D.-Y.; Gong, M.; Chou, H.-L.; Pan, C.-J.; Chen, H.-A.; Wu, Y.; Lin, M.-C.; Guan, M.; Yang, J.; Chen, C.-W. Highly Active and Stable Hybrid Catalyst of Cobalt-Doped FeS_2 Nanosheets-Carbon Nanotubes for Hydrogen Evolution Reaction. *Am. Chem. Soc.* **2015,** *137*, 1587-1592.
24. Xu, Y.; Wu, R.; Zhang, J.; Shi, Y.; Zhang, B. Anion-Exchange Synthesis of Nanoporous FeP Nanosheets as Electrocatalysts for Hydrogen Evolution Reaction. *Chem. Commun.* **2013**, *49*, 6656-6658.
25. Cao, B.; Veith, G. M.; Neuefeind, J. C.; Adzic, R. R.; Khalifah, P. G. Mixed Close-Packed Cobalt Molybdenum Nitrides as Non-Noble Metal Electrocatalysts for the Hydrogen Evolution Reaction. *J. Am. Chem. Soc.* **2013**, *135*, 19186-19192.
26. Zou, X.; Huang, X.; Goswami, A.; Silva, R.; Sathe, B. R.; Mikmeková, E.; Asefa, T. Cobalt-Embedded Nitrogen-Rich Carbon Nanotubes Efficiently Catalyze Hydrogen Evolution Reaction at All pH Values. *Angew. Chem.* **2014**, *126*, 4461-4465.
27. Peng, Z.; Jia, D.; Al-Enizi, A. M.; Elzatahry, A. A.; Zheng, G. Electrocatalysts: from Water Oxidation to Reduction: Homologous Ni-Co Based Nanowires as Complementary Water Splitting Electrocatalysts. *Adv. Energy Mater.* **2015**, *5*, 1402031.
28. Liu, D.; Lu, Q.; Luo, Y.; Sun, X.; Asiri, A. M. $NiCo_2S_4$ Nanowires Array as An Efficient Bifunctional Electrocatalyst for Full Water Splitting with Superior Activity. *Nanoscale* **2015**, *7*, 15122-15126.
29. Jin, H.; Wang, J.; Su, D.; Wei, Z.; Pang, Z.; Wang, Y. In Situ Cobalt-Cobalt Oxide/N-Doped Carbon Hybrids as Superior Bifunctional Electrocatalysts for Hydrogen and Oxygen Evolution. *J. Am. Chem. Soc.* **2015**, *137*, 2688-2694.
30. Stern, L.-A.; Feng, L.; Song, F.; Hu, X. Ni_2P as A Janus Catalyst for Water Splitting: the Oxygen Evolution Activity of Ni_2P Nanoparticles. *Energy Environ. Sci.* **2015**, *8*, 2347-2351.
31. Luo, J.; Im, J.-H.; Mayer, M. T.; Schreier, M.; Nazeeruddin, M. K.; Park, N.-G.; Tilley, S. D.; Fan, H. J.; Grätzel, M. Water Photolysis at 12.3% Efficiency via Perovskite Photovoltaics and Earth-Abundant Catalysts. *Science* **2014**, *345*, 1593-1596.
32. Wu, H. B.; Xia, B. Y.; Yu, L.; Yu, X.-Y.; Lou, X. W. D. Porous Molybdenum Carbide Nano-Octahedrons Synthesized via Confined Carburization in Metal-Organic Frameworks for Efficient Hydrogen Production. *Nat. Commun.* **2015**, *6*, 6512.
33. Yang, Y.; Fei, H.; Ruan, G.; Xiang, C.; Tour, J. M. Efficient Electrocatalytic Oxygen Evolution on Amorphous Nickel-Cobalt Binary Oxide Nanoporous Layers. *ACS Nano* **2014**, *8*, 9518-9523.
34. Shen, M.; Ruan, C.; Chen, Y.; Jiang, C.; Ai, K.; Lu, L. Covalent Entrapment of Cobalt-Iron Sulfides in N-Doped Mesoporous Carbon: Extraordinary Bifunctional Electrocatalysts for Oxygen Reduction and Evolution Reactions. *ACS Appl. Mater. Interfaces* **2015**, *7*, 1207-1218.
35. Ni, B.; Wang, X. Edge Overgrowth of Spiral Bimetallic Hydroxides Ultrathin-Nanosheets for Water Oxidation. *Chem. Sci.* **2015**, *6*, 3572-3576.
36. Liang, H.; Meng, F.; Cabán-Acevedo, M.; Li, L.; Forticaux, A.; Xiu, L.; Wang, Z.; Jin, S. Hydrothermal Continuous Flow Synthesis and Exfoliation of NiCo Layered Double Hydroxide Nanosheets for Enhanced

Oxygen Evolution Catalysis. *Nano Lett.* **2015**, *15*, 1421-1427.

37. Li, Y.; Hasin, P.; Wu, Y. $Ni_xCo_{3-x}O_4$ Nanowire Arrays for Electrocatalytic Oxygen Evolution. *Adv. Mater.* **2010**, *22*, 1926-1929.
38. Hu, H.; Guan, B.; Xia, B.; Lou, X. W. Designed Formation of $Co_3O_4/NiCo_2O_4$ Double-Shelled Nanocages with Enhanced Pseudocapacitive and Electrocatalytic Properties. *J. Am. Chem. Soc.* **2015**, *137*, 5590-5595.
39. Landon, J.; Demeter, E.; Inoğlu, N.; Keturakis, C.; Wachs, I. E.; Vasić, R.; Frenkel, A. I.; Kitchin, J. R. Spectroscopic Characterization of Mixed Fe-Ni Oxide Electrocatalysts for the Oxygen Evolution Reaction in Alkaline Electrolytes. *ACS Catal.* **2012**, *2*, 1793-1801.
40. Liu, Y.; Cheng, H.; Lyu, M.; Fan, S.; Liu, Q.; Zhang, W.; Zhi, Y.; Wang, C.; Xiao, C.; Wei, S. Low Overpotential in Vacancy-Rich Ultrathin $CoSe_2$ Nanosheets for Water Oxidation. *J. Am. Chem. Soc.* **2014**, *136*, 15670-15675.
41. Song, F.; Hu, X. Exfoliation of Layered Double Hydroxides for Enhanced Oxygen Evolution Catalysis. *Nat. Commun.* **2014**, *5*, 4477.
42. Jiang, N.; You, B.; Sheng, M.; Sun, Y. Electrodeposited Cobalt-Phosphorous-Derived Films as Competent Bifunctional Catalysts for Overall Water Splitting. *Angew. Chem. Int. Ed.* **2015**, *54*, 6251-6254.
43. Song, F.; Hu, X. Ultrathin Cobalt-Manganese Layered Double Hydroxide is An Efficient Oxygen Evolution Catalyst. *J. Am. Chem. Soc.* **2014**, *136*, 16481-16484.